Noise Considerations When Determining Phase of Large-Signal Microwave Measurements

Peter Stuart Blockley, *Student Member, IEEE*, Jonathan Brereton Scott, *Senior Member, IEEE*, Daniel Gunyan, *Member, IEEE*, and Anthony Edward Parker, *Senior Member, IEEE*

***Abstract*—Advances in microwave instrumentation now make it feasible to accurately measure not only the magnitude spectrum, but also the phase spectrum of wide-bandwidth signals. In a practical measurement, the spectrum is measured over a finite window of time. The phase spectrum is related to the position of this window, causing the spectrum to differ between measurements of an identical waveform. It is difficult to compare multiple measurements with different window positions or to incorporate them into a model. Several methods have been proposed for determining the phase spectrum such that multiple measurements can be effectively compared and utilized in models. The methods are reviewed in terms of the information required to determine the phase and compared in terms of their robustness in the presence of measurement noise.**

***Index Terms*—Intermodulation distortion, measurement uncertainty, nonlinear systems, phase measurement.**

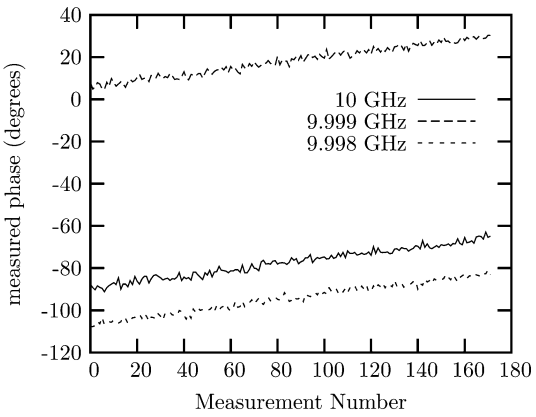

Fig. 1. Phase measurement repeated over a period of time (less than 1 h) for three tones in a multitone signal. Although the sources and measurement system are phase locked to a common reference, the measured phase varies slowly over time due to drift and imperfect phase locking in the system.

I. Introduction

OFTEN nonlinear systems are characterized only by their magnitude spectrum. For instance, verifying spectral mask compliance or determining the third-order intercept point of an amplifier only requires magnitude information. For advanced applications, such as device modeling and linearization, the phase spectrum provides important information and can be readily obtained over wide bandwidths with equivalent-time sampling oscilloscopes or nonlinear network analyzers [1], [2].

The magnitude spectrum of a periodic signal does not depend on the starting time of the time-domain window because the spectrum is independent of time shift. This property allows straightforward comparison of measurements made at different times.

The phase spectrum is dependent on the relative starting time of the time-domain window, making it difficult to compare measurements, or incorporate several measurements made with different starting times into a model. The Fourier transform of a time-shifted waveform, expressed in terms of magnitude and phase, is

$$f(t+t_0) \leftrightarrow F(\omega)e^{j\omega t_0} \leftrightarrow |F(\omega)|\angle(\arg[F(\omega)] + \omega t_0) \quad (1)$$

where $f(t+t_0)$ is a time-domain function with time shift of t_0, $F(\omega)$ is the corresponding frequency spectrum, ω is the angular frequency, and $\arg(x)$ is the argument of x (the angle associated with the complex quantity x).

The difficulty is in finding the relative time shift between two measurements made at different times in the presence of measurement noise and without an absolute time-reference. Fig. 1 is an example of a phase measurement using the large-signal network analyzer (LSNA) system described in [2] repeated over a period of time. The measurements are before any processing and may differ from those obtained by other LSNA instruments, such as [1], published in the literature. The phase varies slowly over time due to drift and imperfect phase locking in the system. Note that while the measured phase appeared to follow a linear trend, consistent with a phase lock drift, this is not always the case.

In linear systems, the issue is resolved by extracting a linear time-invariant model. For measurements of nonlinear systems, *alignment methods* and *time-zero cancellation* methods have been proposed for determining the phase. Alignment methods seek to align the measured signal to an explicit target signal, while time-zero cancellation methods seek to cancel t_0 in (1) through a linear transformation of the measured phase values.

Manuscript received December 15, 2005; revised May 12, 2006.

P. S. Blockley and A. E. Parker are with the Department of Electronics, Macquarie University, Sydney, N.S.W. 2109, Australia (e-mail: peterblockley@ieee.org).

J. B. Scott was with the Microwave Technology Center, Agilent Technologies, Santa Rosa, CA 95404 USA. He is now with the School of Science and Engineering, University of Waikato, Hamilton, New Zealand (e-mail: jonathanscott@ieee.org).

D. Gunyan is with the Microwave Technology Center, Agilent Technologies, Santa Rosa, CA 95404 USA (e-mail: daniel.gunyan@ieee.org).

Digital Object Identifier 10.1109/TMTT.2006.879136

While a variety of phase processing methods have been reported in the literature, the consequences of measurement noise on the variance of the transformed phase is often not considered. However, it has been noted that different alignment methods can result in different uncertainties [3] and a study of time-domain methods for aligning noisy signals was conducted in [4].

This paper provides analysis of the uncertainty in the time-zero cancellation methods and a comparison with the alignment methods using real measurements. It shows that the time-zero cancellation methods have a variance that can change significantly across the measurement bandwidth. The covariance matrix for the time-zero cancellation method is derived and can be used when the transformed measurements are used for developing models.

Section II describes the extraction of linear time-invariant models for linear systems. Section III gives an overview of phase-determining methods that have been proposed for systems with energy at the fundamental frequency, and Section IV gives an overview of phase-determining methods that have been proposed for systems without energy at the fundamental frequency. The methods are presented in a historical order such that the reader may gain insight into the development of this theory. Section V derives the covariance matrix for the time-zero cancellation method. Section VI presents measurement examples using some of the methods described in Section IV.

II. Linear Systems

In linear systems, the phase-determination problem is often resolved by extracting a linear time-invariant model. The output $b(t)$ of a linear time-invariant system as a function of input $a(t)$ is given by

$$b(t+t_0) = \int_{-\infty}^{\infty} h(\tau)a(t+t_0-\tau)\,d\tau \tag{2}$$

where t is the time and $h(\tau)$ is the system's impulse response.

This definition is useful because $h(\tau)$ does not depend on t_0, even though the signals $a(t)$ and $b(t)$ do.

Applying the Fourier transform to both sides of (2) gives

$$B(\omega) = H(\omega)A(\omega). \tag{3}$$

where $A(\omega), B(\omega)$, and $H(\omega)$ are the Fourier transforms of $a(t), b(t)$, and $h(\tau)$ respectively.

A discrete version of $H(\omega)$ is, therefore, easily extracted in the frequency domain using a vector network analyzer. A discrete frequency-domain model that uses the extracted data is a finite state moving average model in the time domain and has well-understood limitations.

If the measurements of the phase $\varphi[A(\omega)]$ and $\varphi[B(\omega)]$ are independent, then the variance of $\varphi[H(\omega)]$ is

$$\mathrm{var}[\varphi[H(\omega)]] = \mathrm{var}[\varphi[A(\omega)]] + \mathrm{var}[\varphi[B(\omega)]] \tag{4}$$

where $\mathrm{var}(x)$ is the variance of the variable x and $\varphi(x)$ is a function that returns the argument of x (the angle associated with the complex quantity of x).

The model has the property that if the variance of $\varphi[A(\omega)]$ and $\varphi[B(\omega)]$ are statistically independent and do not change with frequency, then the variance of $\varphi[H(\omega)]$ is statistically independent and does not change with frequency.

Nonlinear system theory currently does not offer such a practical solution. Nonlinear time-series models, which are an extension of the linear moving average and autoregressive moving average models are possible, but a nonlinear system can have many states that depend on both time and amplitude. Unlike the linear case, it is difficult to excite every state in a nonlinear system and the large number of states can make the model computationally large.

III. Nonlinear System-Fundamental Tone Present

A simple case is one where the signals of interest contain energy at the fundamental frequency. The signal-alignment process is easier because the phase of the fundamental rotates through 360° once only, over one period of the signal. This section gives an overview of time-domain signal alignment, fundamental alignment, frequency-domain alignment, and time-zero cancellation methods when the fundamental tone is present.

A. Time-Domain Signal Alignment

The goal of signal alignment is to calculate the relative time shift between signals. The simplest method is to calculate the time shift between a measured and a target signal.

Ideally the measured signal is a time-delayed version of the target signal that has been corrupted by Gaussian noise. The first measurement can be used as the target signal (as is done in this paper) or estimated from multiple measurements [5]. When calculating relative time shift between three or more signals, the "complete cross-correlation" method has been shown to be the most accurate [4].

One method is to maximize the cross-correlation of the measured and target signal, i.e., to maximize

$$f \star g = \int_{-\infty}^{\infty} f(\tau)g(t+\tau)\,d\tau \tag{5}$$

which is the cross-correlation of the target signal $f(t)$ and measured signal $g(t)$.

This is a nonlinear problem without an explicit solution and can be difficult to solve due to a large number of local maximums. The signal-alignment algorithm used in the comparative study [4] used a golden section search and parabolic interpolation to evaluate the local minimums of the error function in search of the global solution.

For multiport systems, the signal-alignment method might be applied only to the incident wave and the other ports time shifted accordingly. This might be useful, for example, for observing changes in phase over bias in a transistor.

The advantage of signal alignment is its good immunity to measurement noise. The method requires an explicit target

signal. A distorted target signal (random noise, linear/nonlinear distortion, or systematic error) can have an effect on the variance and correctness of the assumptions.

B. Fundamental Alignment

In many situations, the target signal and corresponding phases may not be known. Fundamental alignment is a method that requires an arbitrary choice of target phase and has an explicit solution. The fundamental can be aligned to an arbitrary phase (this paper will consider the alignment of the fundamental phase to 0°) without consideration of the harmonic frequencies. An explicit solution was formally considered by Jargon *et al.* [6], but had been previously implemented in LSNA software by Verspecht and Vanden Bossche for visualization purposes only [7].

Consider signal components at frequencies f_i with phases Φ_i, where f_0 is the fundamental frequency of the spectrum and Φ_0 is the measured phase at the fundamental frequency. The aligned phase of the component at f_i, denoted Φ_i', is given by

$$\begin{aligned}\Phi_i^{'} &= (\Phi_i + 2\pi f_i t_0) - \frac{f_i}{f_0}(\Phi_0 + 2\pi f_0 t_0) \\ &= \Phi_i - \frac{f_i}{f_0}\Phi_0 \end{aligned} \tag{6}$$

where $f_i = (i+1)f_0$, i is an integer ($i \geq 0$), and the phases are modulo 2π (i.e., $0 \leq \Phi < 2\pi$). Note that $\Phi_0' = 0$.

It is interesting to note that an arbitrary t_0 does not affect the aligned phase $\Phi_i^{'}$ and is referred to as "time-invariant phase" in [6]. This invariance to t_0 is the basis of time-zero cancellation discussed below.

Now consider the variance (or combined uncertainty [8]) assuming that the frequency relationship is perfectly known and $i \geq 1$

$$\begin{aligned}\mathrm{var}(\Phi_i^{'}) &= \mathrm{var}(\Phi_i - \frac{f_i}{f_0}\Phi_0) \\ &= \mathrm{var}(\Phi_i) + \left(\frac{f_i}{f_0}\right)^2 \mathrm{var}(\Phi_0) - 2\frac{f_i}{f_0}\mathrm{cov}(\Phi_0, \Phi_i)\end{aligned} \tag{7}$$

where $\mathrm{cov}(x, y)$ is the covariance of the variables x and y.

If the variance of the measurements of Φ_0 and Φ_i are due to independent processes, then the covariance can be assumed zero. Therefore, for large values of f_i/f_0, the aligned phase will have significantly greater variance than the measured phase.

For multiport systems, the fundamental alignment method might be applied only to the incident wave and the other ports time shifted accordingly.

C. Frequency-Domain Alignment

Frequency-domain alignment estimates a time t_0 when the phases align. This was formally considered in [9] and called "phase detrending." The method is very similar to signal alignment and is referred to here as frequency-domain alignment. The signal-alignment method presented in Section III-A is performed in the time domain by maximizing the cross-correlation of the measured and target signal. Frequency-domain alignment considered in [9] is performed by minimizing the least squared error between the measured and target phases.

The choice of target signal/phases will depend on the application. In this paper, the target phases are chosen to be the first measurement, but various (often superior) approaches can be used for estimating the target signal from the measurement data [4]. Alternatively, the target phases could be those programed into the signal generator or from another port in a multiport system [9]. Care must be taken when selecting the target signal, as distortion can increase the observed variance.

For aligning measurements that contain noise, a least squares or a weighted least squares problem is formulated. When the phase measurements have equal variance, the least squares problem is to minimize the error function

$$E(t) = \sum_{i=1}^{N} |\theta_i(t) - \theta_{i,\mathrm{target}}|^2 \tag{8}$$

where t is the time shift, $\theta_i(t)$ is a vector of phases with index i, and $\theta_{i,\mathrm{target}}$ is the vector of target phases with index i.

Frequency-domain alignment is closely related to time-domain signal alignment. In fact, the solutions converge to the same t_0 estimate when the signals perfectly align.

To demonstrate this, consider that the real-valued time-domain signals to be aligned consist of a discrete set of tones. Noting the Fourier transform pair $f \star g \leftrightarrow F(-\omega)G(\omega)$, the time-domain signal-alignment problem is that of maximizing a Fourier series

$$f \star g = \sum_{i=-N}^{N} F(-\omega_i)G(\omega_i)e^{j\omega_i t} \tag{9}$$

$$= \sum_{i=-N}^{N} (A_i' e^{-j\phi_i'} A_i'' e^{j\phi_i''})e^{j\omega_i t} \tag{10}$$

$$= A_0' A_0'' + \sum_{i=1}^{N} 2A_i' A_i'' \cos(\phi_i'' - \phi_i' + \omega_i t) \tag{11}$$

where $e^{j\phi_{-i}} = e^{-j\phi_i}$, $A'_{-i} = A_i'$, $A''_{-i} = A_i''$, and A_i' is the amplitude of the target $f(t)$, ϕ_i' is the phase of the target $f(t)$, A_i'' is the amplitude of the measured signal $g(t)$, and ϕ_i'' is the phase of the measured signal $g(t)$.

If the signals align perfectly, then at the solution, $(\phi_i'' - \phi_i' + \omega_i t)$ modulo 2π must be zero. Expanding $\cos(x)$ at the solution when the signals align perfectly ($x = \ldots, -2\pi, 0, 2\pi, \ldots$) in a Taylor series truncated to the second order ($\cos[x] \approx 1 - 1/2x^2$) and substituting gives

$$f \star g \approx A_0' A_0'' + \sum_{i=1}^{N} A_i' A_i'' \left(2 - [\theta_i(t) - \phi_i']^2\right) \tag{12}$$

$$\approx \sum_{i=-N}^{N} A_i' A_i'' - \sum_{i=1}^{N} A_i' A_i'' |\theta_i(t) - \theta_{i,\mathrm{target}}|^2 \tag{13}$$

where $\theta_i(t) = (\phi_i'' + \omega_i t)$ modulo 2π (i.e., $0 \leq \theta_i(t) < 2\pi$).

Maximization of $f \star g$ is equivalent to minimization of $-f \star g$. Therefore, the solution of time-domain signal-alignment converges to the solution of the frequency-domain alignment problem (8) when the tones have equal magnitude and the signals are perfectly aligned.

Frequency-domain alignment has the same advantage as signal alignment, i.e., that of good immunity to measurement noise. Both the time-domain signal-alignment and frequency-domain alignment methods require explicit target phases of the signal to be measured.

The time-domain signal alignment implicitly weights the error function in proportion to the magnitude squared of the frequency components. This weighting may be correct for many systems where the variance of the phase is inversely proportional to the magnitude squared of the signal, but this is not the case for the LSNA presented in [2]. Frequency-domain alignment does not make any assumptions about the weights, hence, an appropriately weighted version of (8) would be expected to perform better in a broad range of measurement systems.

D. Time-Zero Cancellation

The high uncertainty in the fundamental alignment method described in Section III-B has lead to development of methods to reduce the propagation of errors for some measurement scenarios. The signal-alignment methods seek to estimate t_0 then align the signal to time zero (a point where $t_0 = 0$). Time-zero cancellation applies a linear transform to the phase such that the new phase values are not dependent on t_0 [10].

Consider expressing a frequency $f_{k,m}$ as

$$f_{k,m} = kf_c + mf_0 \tag{14}$$

where k and m are the integer coefficients in a linear combination of the carrier frequency f_c and frequency f_0.

The time-zero cancellation phase at frequency $f_{k,m}$ is defined as

$$\Phi'_{k,m} = \Phi_{k,m} - (k\Phi_c + m\Phi_0) \tag{15}$$

where $\Phi_{k,m}$ is the measured phase at $f_{k,m}$, Φ_c is the measured phase at the carrier frequency, and Φ_0 is the measured phase at the fundamental frequency.

Assuming the variance of the measurement is not correlated across frequency, the variance of the time-zero cancellation phase is given by

$$(\sigma'_{k,m})^2 = \begin{cases} 0, & \text{if } k = 0, m = 1 \\ 0, & \text{if } k = 1, m = 0 \\ \sigma^2_{k,m} + k^2\sigma_c^2 + m^2\sigma_0^2, & \text{otherwise} \end{cases} \tag{16}$$

where $(\sigma'_{k,m})^2$ is the variance of the time-zero cancellation phase $\Phi'_{k,m}$, $\sigma^2_{k,m}$ is the variance of the measured phase $\Phi_{k,m}$, and σ_c^2 is the variance of the measured phase Φ_c at the carrier frequency.

Therefore, when the carrier frequency f_c is much greater than the frequency f_0, the variance of the time-zero cancellation method is significantly less than the variance of the fundamental alignment method (7) because k and m are typically much less than i. Similar to the fundamental alignment method, the time-zero cancellation method only requires arbitrary selected target phases.

For a mixer application, the carrier frequency f_c might exist at the local-oscillator port and the frequency f_0 at the IF port. The time-zero cancellation method might be applied to the RF port using Φ_c from the local-oscillator port and Φ_0 from the IF port. For multiport applications, the variance will differ from that derived in (16).

IV. Nonlinear System-Fundamental Suppressed

Often a multitone signal has no energy at the fundamental frequency. The methods presented in Section III can be applied to nonlinear systems where the fundamental tone is not present with little or no modification. An overview of time-domain signal-alignment, frequency-domain alignment, two-tone envelope alignment (equivalent to fundamental alignment, but for the case when the fundamental is suppressed) and time-zero cancellation methods when the fundamental tone is suppressed or not present is presented here.

A. Time/Frequency-Domain Alignment

Time-domain signal alignment with a suppressed fundamental is the same as in Section III-A. The case is typically more difficult to solve due to the large number of local maximums with very close maximum values. This is because the tones of the signal traverse many 360° cycles over one period.

Frequency-domain alignment with a suppressed fundamental tone is the same as in Section III-C. The case is typically more difficult to solve due to the large number of local minimums with very close minimum values.

Consider the example of ten unity magnitude tones evenly spaced from 1 to 1.09 GHz. Each tone of the measured signal has a phase of 0° and the target signal is the same, but time shifted by 0.5 ns. A graphical example of the time-domain signal-alignment error function (inverted and with an offset) and frequency-domain alignment error function are shown in Fig. 2. The error functions have many local extreme points. The signals align perfectly at $t = 0.5$ ns, the global solution to both error functions.

B. Two-Tone Envelope Alignment

Two-tone envelope alignment is an extension of the fundamental alignment method from Section III-B. When signals are considered that have no energy at the fundamental frequency f_0, Φ_0 can be redefined as the difference in phase of two adjacent reference frequency components ($k = 1, m = 0$, and $m = -1$). The phase of the envelope of the two-tone signal is then Φ_0. This effectively sets the phase difference of two adjacent frequencies to a fixed value. In this paper, the phase difference is set to zero, but could be set to an arbitrary target phase difference. Two-tone envelope alignment was first used as part of a derivation for the initial estimate of the frequency-domain alignment solution [9].

Letting $\Phi_0 = \Phi_c - \Phi_{1,-1}$, then

$$\Phi'_{k,m} = \Phi_{k,m} - \frac{f_{k,m}}{f_0}(\Phi_c - \Phi_{1,-1}) \tag{17}$$

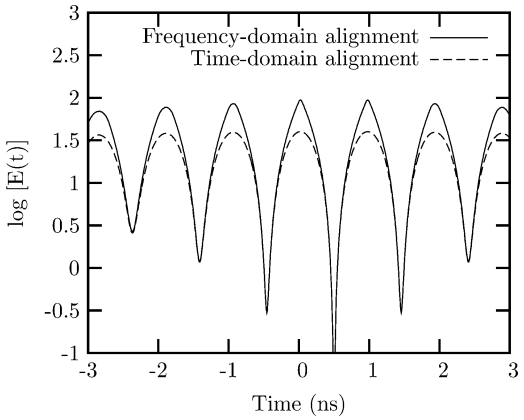

Fig. 2. Example plot of the frequency-domain alignment error function $E(t)$ and the time-domain alignment error function $-f \star g + 20$. The error functions typically have many local extreme points, which makes evaluation of the global minimum difficult. This is an example of ten tones evenly spaced from 1 to 1.09 GHz with unity magnitude. There is no noise in this example, therefore, there is an exact solution $E(t) = 0$ and $-f \star g + 20 = 0$ to both problems at $t = 0.5$ ns. The minimum value of the function $\log[E(t)]$ is much less than -1, but is not shown due to truncation of the y-axis.

where $\Phi'_{k,m}$ is the aligned phase at the frequency $f_{k,m}$ and $\Phi_{k,m}$ is the measured phase at $f_{k,m}$, Φ_c is the measured phase at the carrier frequency and $\Phi_{1,-1}$ is the measured phase at the lower adjacent frequency.

Consider the variance assuming that the frequency relationship is perfectly known and the phase measurements are independent as follows:

$$(\sigma'_{k,m})^2 = \begin{cases} \left(\frac{f_{k,m}}{f_0} - 1\right)^2 \sigma_c^2 + \frac{f_{k,m}^2}{f_0^2}\sigma_{1,-1}^2, & k = 1, m = 0 \\ \frac{f_{k,m}^2}{f_0^2}\sigma_c^2 + \left(\frac{f_{k,m}}{f_0} + 1\right)^2 \sigma_{1,-1}^2, & k = 1, m = -1 \\ \sigma_{k,m}^2 + \frac{f_{k,m}^2}{f_0^2}\sigma_c^2 + \frac{f_{k,m}^2}{f_0^2}\sigma_{1,-1}^2, & \text{otherwise.} \end{cases} \tag{18}$$

The resulting variance of the two-tone envelope alignment phase can be significantly greater than the variance of the measured phase in certain applications. Consider the measurement of the phase of the third-order intermodulation product (IM_3) in a two-tone test. The variance of the aligned phase would be significantly greater than the measured phase when the tone spacing is small. Consider a two-tone test with tones at 1 GHz [$f_{(1,-1)}$] and 1.001 GHz (f_c), where the variance of the measured phase $\sigma_{k,m}$ is equal and independent across frequency. For this example, the variance of the aligned IM_3 phase Φ'_i would be more than 60 dB greater than the variance of the measured IM_3 phase Φ_i.

C. Time-Zero Cancellation

Cancellation of time zero when the fundamental is suppressed is an extension of the time-zero cancellation method presented in Section III-D. The phase of the fundamental Φ_0 is chosen to be the difference in phase between two adjacent reference tones ($k = 1$, $m = 0$, and $m = -1$). This effectively sets the phase of two adjacent tones to a fixed value. In this paper, the phases of the two adjacent tones are set to zero, but could be set to any arbitrary target phases. This technique was first investigated for two-tone intermodulation distortion by [11] and further by [12] and [10].

Letting $\Phi_0 = \Phi_c - \Phi_{(1,-1)}$ and expanding (15), for this case gives

$$\Phi'_{k,m} = \Phi_{k,m} - (k+m)\Phi_c + m\Phi_{(1,-1)}. \tag{19}$$

The time-zero cancellation phase can be considered as the phase deviation from a "reference nonlinearity" excited with the adjacent reference tones [12]. For IM_3 measurements, the "reference nonlinearity" might be the following:

$$\mathrm{ref}(x) = x + x^3. \tag{20}$$

Expanding the reference nonlinearity (20) for the fundamental and IM_3 distortion products, where $x = A_1\cos(2\pi f_c t + \Phi_c) + A_2\cos(2\pi f_{(1,-1)}t + \Phi_{(1,-1)})$ gives

$$\begin{aligned} v(t) = {} & A'_c\cos(2\pi f_c t + \Phi_c) \\ & + A'_{(1,-1)}\cos(2\pi f_{(1,-1)}t + \Phi_{(1,-1)}) \\ & + A'_{(1,-2)}\cos(2\pi f_{(1,-2)}t + 2\Phi_{(1,-1)} - \Phi_c) \\ & + A'_{(1,1)}\cos(2\pi f_{(1,1)}t + 2\Phi_c - \Phi_{(1,-1)}) \\ & + \ldots \end{aligned} \tag{21}$$

where A'_1, A'_2, $A'_{(1,-2)}$, and $A'_{(1,1)}$ are the amplitudes of the reference distortion $v(t)$ generated from the reference nonlinearity $\mathrm{ref}(x)$.

Subtracting the phase of the reference distortion from the measured phase for each corresponding frequency gives the time-zero cancellation phase. For the IM_3 distortion example, the time-zero cancellation phases are

$$\begin{bmatrix} \Phi'_{1,-2} \\ \Phi'_{1,-1} \\ \Phi'_{1,0} \\ \Phi'_{1,1} \end{bmatrix} = \begin{bmatrix} 1 & -2 & 1 & 0 \\ 0 & 0 & 0 & 0 \\ 0 & 0 & 0 & 0 \\ 0 & 1 & -2 & 1 \end{bmatrix} \begin{bmatrix} \Phi_{1,-2} \\ \Phi_{1,-1} \\ \Phi_{1,0} \\ \Phi_{1,1} \end{bmatrix}. \tag{22}$$

The time-zero cancellation method (19) is equivalent to signal alignment only when the following holds:

$$\left[\Phi_c\frac{f_{(1,-1)}}{f_0} - \Phi_{(1,-1)}\frac{f_c}{f_0}\right] \text{modulo } 2\pi = 0. \tag{23}$$

Therefore, time-zero cancellation cannot be regarded generally as a signal-alignment method and care must be taken when using data transformed in this way. Alternatively, an alignment method can be used to align the phases of two adjacent frequency components to their corresponding explicit target phases. This was considered in [9] as a starting estimate for the frequency-domain alignment problem.

Assuming the variance of the measurement is not correlated across frequency, the variance of the time-zero cancellation phase is given by

$$(\sigma'_{k,m})^2 = \begin{cases} 0,, & k=1, m=0 \\ 0, & k=1, m=-1 \\ \sigma^2_{k,m}+(k+m)^2\sigma_c^2+m^2\sigma^2_{(1,-1)}, & \text{otherwise.} \end{cases} \tag{24}$$

Using the previous two-tone example from Section IV-B of a 1-GHz [$f_{(1,-1)}$] and a 1.001-GHz (f_c) tone, the variance of the phase of the IM_3 increases by less than 8 dB. Thus, this method is suitable for narrowband modulations, but is not suitable for wide-bandwidth applications. For the example shown in [13], a multitone signal was generated with 800-MHz bandwidth, carrier frequency of 3.66 GHz, and fundamental of 1.8 MHz. The resulting variance of the time-zero cancellation phase would be up to 48 dB greater than the measured phase for some frequency components in the signal.

For a multiport system, Φ_c and $\Phi_{(1,-1)}$ would typically be taken from the incident wave and the time-zero cancellation applied to all ports. References [11] and [12] give examples of a two-port excited by a two-tone excitation.

V. Covariance Matrix for Time-Zero Cancellation

Phase determination using time-zero cancellation has been suggested for modeling applications [10]. At first glance, the method appears to simplify the fitting of models, but the method introduces correlation in the phase across frequency, which must be taken into consideration.

Take an example of a four-tone signal ($N=4$). If the measurements of the phase are independent with equal variance, then the covariance matrix Σ for the measured phase would be

$$\Sigma = \begin{bmatrix} \sigma^2 & 0 & 0 & 0 \\ 0 & \sigma^2 & 0 & 0 \\ 0 & 0 & \sigma^2 & 0 \\ 0 & 0 & 0 & \sigma^2 \end{bmatrix} \tag{25}$$

where σ^2 is the variance of the measured phase.

If the individual phases have Gaussian distribution, then the multivariate Gaussian (normal) distribution is given by

$$f(\Phi) = \frac{1}{\sqrt{(2\pi)^N|\Sigma|}} \exp\left[-\frac{1}{2}(\Phi - M)^T\Sigma^{-1}(\Phi - M)\right] \tag{26}$$

where Φ is the vector of phases $(\phi_1, \phi_2, \phi_3, \phi_4)^T$ and M is the vector of mean values $(\mu_1, \mu_2, \mu_3, \mu_4)^T$ corresponding to the elements in Φ, and N is the number of elements in Φ.

To compute the covariance matrix for the time-zero cancellation phase (19), the multivariate Jacobian matrix is first computed (which corresponds to the transfer function since the time-zero cancellation phase is a linear transform)

$$\frac{\partial\Phi'}{\partial\Phi} = \begin{bmatrix} \frac{\partial\phi'_1}{\partial\phi_1} & \frac{\partial\phi'_1}{\partial\phi_2} & \frac{\partial\phi'_1}{\partial\phi_3} & \frac{\partial\phi'_1}{\partial\phi_4} \\ \frac{\partial\phi'_2}{\partial\phi_1} & \frac{\partial\phi'_2}{\partial\phi_2} & \frac{\partial\phi'_2}{\partial\phi_3} & \frac{\partial\phi'_2}{\partial\phi_4} \\ \frac{\partial\phi'_3}{\partial\phi_1} & \frac{\partial\phi'_3}{\partial\phi_2} & \frac{\partial\phi'_3}{\partial\phi_3} & \frac{\partial\phi'_3}{\partial\phi_4} \\ \frac{\partial\phi'_4}{\partial\phi_1} & \frac{\partial\phi'_4}{\partial\phi_2} & \frac{\partial\phi'_4}{\partial\phi_3} & \frac{\partial\phi'_4}{\partial\phi_4} \end{bmatrix} = \begin{bmatrix} 1 & -2 & 1 & 0 \\ 0 & 0 & 0 & 0 \\ 0 & 0 & 0 & 0 \\ 0 & 1 & -2 & 1 \end{bmatrix}. \tag{27}$$

The covariance matrix Σ' of quantities after the time-zero cancellation transform is applied is given by (see [14] for a proof)

$$\Sigma' = \frac{\partial\Phi'}{\partial\Phi}\Sigma\left(\frac{\partial\Phi'}{\partial\Phi}\right)^T = \begin{bmatrix} 6\sigma^2 & 0 & 0 & -4\sigma^2 \\ 0 & 0 & 0 & 0 \\ 0 & 0 & 0 & 0 \\ -4\sigma^2 & 0 & 0 & 6\sigma^2 \end{bmatrix}. \tag{28}$$

The time-zero cancellation transform is linear, therefore, this method provides an accurate covariance matrix for the time-zero cancellation phase. From the covariance matrix, an increase in the variance $(6\sigma^2)$ is observed as well as a high correlation $(-4\sigma^2)$ between the first and fourth tones.

Typically the population covariance is not known, thus the sample covariance (V) is used after transformation using (28). A confidence region for the mean vector (M) can then be specified for the measurement as

$$(\Phi - M)^T(V')^{-1}(\Phi - M) \le \frac{2(n-1)}{n-2}F_{2,n-2}(\alpha) \tag{29}$$

where n is the number of samples, Φ is the sample mean vector, V' is the transformed sample covariance matrix, and $F_{2,n-2}(\alpha)$ is the upper 100αth percentile of the F distribution [15].

VI. Measurements

To verify the theoretical derivation for the propagation of measurement error, measurements were taken with the measurement system described in [2]. The signal source, phase reference clock, and the receiver hardware were phase locked via a 10-MHz reference. The phase varies slowly with time, as can be seen in Fig. 1, due to drift and imperfect phase locking. Two measurements were performed: a two-tone measurement and a multitone measurement.

A. Multitone Measurement

The multitone consists of 41 pseudorandom phased tones spaced 1 MHz apart centered around 10 GHz (10-GHz carrier with 20 tones spaced either side), generated with an Agilent E8267C PSG. To calculate the sample variance of the

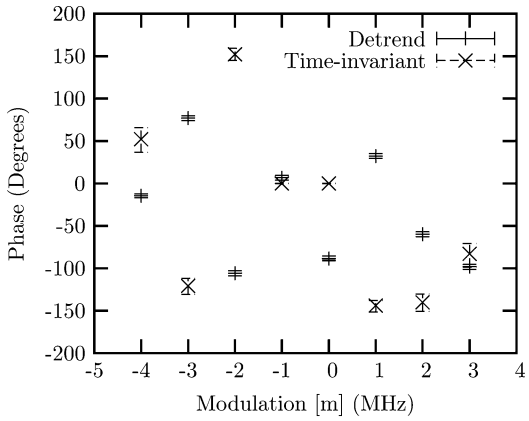

Fig. 3. Time-zero cancellation phase and frequency-domain alignment phase for eight tones of the 41-tone (multitone) signal. The frequency-domain alignment phase and time-zero cancellation phase are represented with an error bar giving the minimum and maximum measured values around a mean. The frequency-domain alignment has fairly constant variance across the frequency range, resulting in fairly constant error bar size. The time-zero cancellation phase is set to zero with zero variance at $k = 1, m = 0$, and $k = 1, m = -1$, and has increasing sample spread for frequencies further away. The mean values of the frequency-domain alignment and time-zero cancellation phases have different values because the frequency-domain alignment is aligned to the first sample, while the time-zero cancellation phase is set to zero at $m = 0$ and $m = -1$.

time-zero cancellation (19) phase, time-domain signal-alignment (5) phase and frequency-domain alignment (8) phase, 172 measurements were performed. The frequency-domain alignment was implemented using MATLAB[1] code from [9] and the time-domain signal-alignment method was implemented using a modified version of the code. The phase of the first measurement is used as the explicit target phase required to align the remaining 171 measurements.

The time-zero cancellation phase and frequency-domain alignment phase for eight tones of the multitone signal are shown in Fig. 3. The frequency-domain alignment phase and time-zero cancellation phase are represented with an error bar giving the minimum and maximum measured values around a mean. The frequency-domain alignment phase has fairly constant variance across the frequency range, resulting in fairly constant error bar size. The time-zero cancellation phase is set to zero with zero variance at the reference frequencies ($k = 1$, $m = 0$, and $k = 1$, $m = -1$) and has increasing sample spread for frequencies further away. The mean values of the frequency-domain alignment and time-zero cancellation phases have different values because the frequency-domain alignment is aligned to the first sample, while the time-zero cancellation phase is set to zero at $m = 0$ and $m = -1$.

The measured standard deviation for the time-zero cancellation phase, calculated standard deviation (24) for the time-zero cancellation phase, measured standard deviation for the frequency-domain alignment, and measured standard deviation for the time-domain signal-alignment are shown in Fig. 4. The calculated standard deviation in the time-zero cancellation phase (24) is evaluated where $\sigma^2_{k,m}$ is the average variance of the frequency-domain alignment phase.

[1]MATLAB is a registered trademark of The MathWorks Inc., Natick, MA.

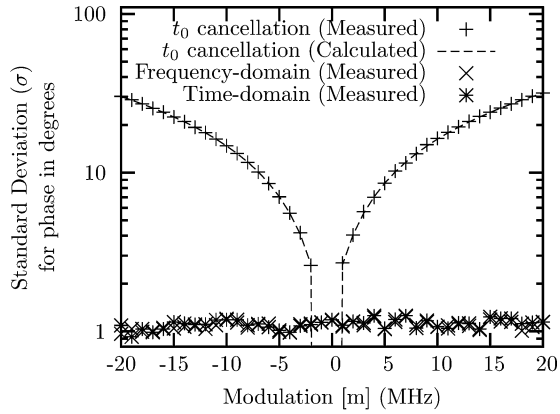

Fig. 4. Comparison between the measured and calculated standard deviation for different tones in a multitone signal when using the time-zero cancellation method. The time-zero cancellation phase is set to zero with zero variance at $k = 1, m = 0$, and $k = 1, m = -1$, and has increasing standard deviation for frequencies further away. The standard deviation in the time-zero cancellation phase is calculated from (24) using the average variance of the frequency-domain alignment phase. This is contrasted with the standard deviation using the time- and frequency-domain alignment methods. The time-zero cancellation results in higher standard deviation compared to the alignment methods, but only requires arbitrary target phases.

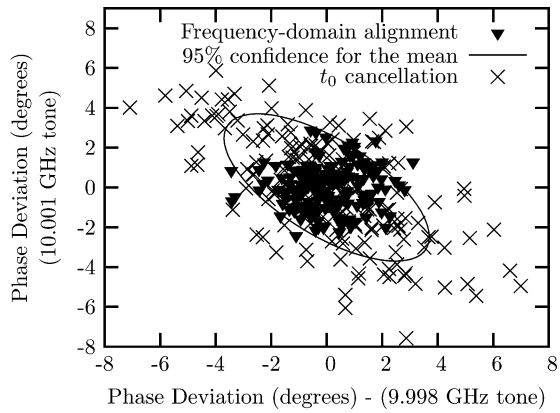

Fig. 5. Phase deviation from the mean of the frequency-domain alignment phase and time-zero cancellation phase for samples of the 9.998-GHz tone against the 10.001-GHz tone. A 95% confidence region (29) for the mean of the time-zero cancellation phase is defined on the plot, where σ^2 is the average variance of the frequency-domain alignment phase. Analysis of multiple tones is possible, but it is difficult to graph more than three tones.

As the presented theory predicts, the time-zero cancellation method amplifies the variance of the underlying measurements used. This increase in variance was quite significant for the multitone measurement considered. The time-domain signal-alignment and frequency-domain alignment methods have significantly lower variance across the bandwidth than the time-zero cancellation method.

Fig. 5 plots the deviation from the mean of the frequency-domain alignment phase and time-zero cancellation phase for samples of the 9.998-GHz tone against the 10.001-GHz tone. This plot clearly shows the high correlation between the tones of the time-zero cancellation phase. This is in contrast to the frequency-domain alignment phase, which has low correlation between the tones. A high correlation in the time-zero cancellation phase is observed between the 9.998- and 10.001-GHz tone because both tones share a component due to the tone at $k = 1$

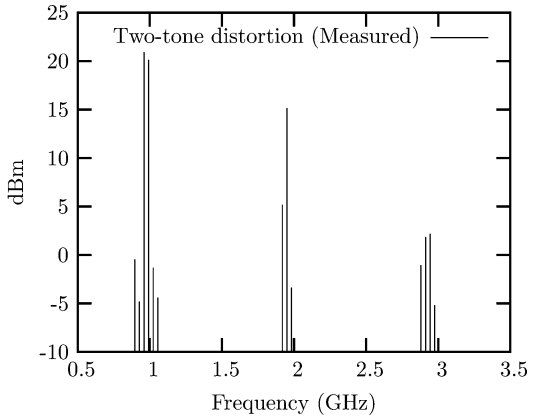

Fig. 6. Measured magnitude spectrum for two-tone test of a Mini-Circuits amplifier. The distortion products have smaller amplitude than the fundamental tones.

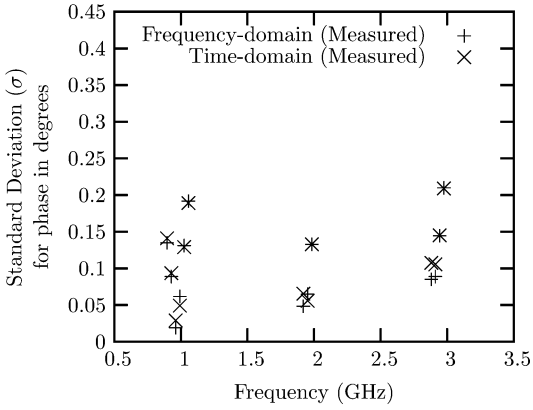

Fig. 7. Comparison of the standard deviation in the phase for the time-domain signal-alignment and frequency-domain alignment methods for the tones in Fig. 6. The frequency-domain alignment problem was weighted by an estimate of the variance of the measured phase.

and $m = -1$. A 95% confidence region (29) for the mean of the time-zero cancellation phase is defined in the plot, where σ^2 is the average variance of the frequency-domain alignment phase.

B. Two-Tone Measurement

For the two-tone measurement, two equal-amplitude tones were generated with an Agilent E8267C PSG and used to drive a Mini-Circuits amplifier. The distortion at the output of the amplifier is shown in Fig. 6.

Comparison of the standard deviation in the phase for the time-domain signal-alignment (5) and frequency-domain alignment (8) methods is shown in Fig. 7. The magnitude of the distortion products is less than the fundamental tones and, thus, the variance of the measured phase cannot be assumed equal. Therefore, the frequency-domain alignment problem was weighted by an estimate of the variance of the measured phase (the variance of the measured phase was estimated by first differencing sequential measurements to remove the trend in the measured data).

The time-zero cancellation phase (19) was calculated with f_c set to 992 MHz and $f_{1,-1}$ to 960 MHz, the fundamental tones

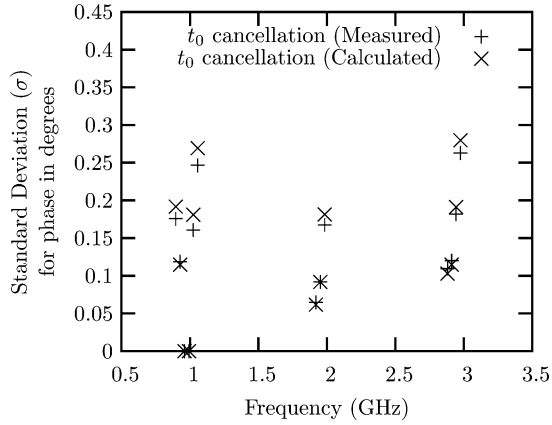

Fig. 8. Comparison of the calculated standard deviation (24) and standard deviation in the measured phase of the time-zero cancellation method for the tones in Fig. 6. The calculated standard deviation (24) was evaluated, where $\sigma^2_{k,m}$ was the variance of the frequency-domain alignment phase.

at the output of the amplifier. The calculated standard deviation (24) and standard deviation in the measured phase for the time-zero cancellation method is shown in Fig. 8. The calculated standard deviation (24) was evaluated, where $\sigma^2_{k,m}$ was the variance of the frequency-domain alignment phase.

The difference in variance between the time-zero cancellation phase and alignment methods is not as significant as in the multitone example because the variance of the phase of the fundamental tones is less than that in the phase of the distortion products. Thus, two-tone distortion measurements are a possible candidate for time-zero cancellation methods, coupled with an appropriate covariance matrix.

VII. Applications

The alignment methods were shown to have good immunity to measurement noise, but require explicit target phase values. Alignment methods can be used to align narrow- or wide-bandwidth multitone signals.

The fundamental alignment and time-zero cancellation methods are appropriate for weakly nonlinear distortion measurements where the variance of the phase for the distortion products is greater than the reference tones. Two-tone amplifier distortion measurements are a good candidate for time-zero cancellation methods, as the increase in variance tends to be small and good models can be extracted when coupled with the correct covariance matrix.

VIII. Conclusion

Several phase determination methods have been evaluated in terms of their performance in the presence of measurement noise. It was found that the alignment methods perform well in the presence of measurement noise, but require explicit target phases. The time-zero cancellation methods do not perform as well in the presence of measurement noise, but only require arbitrary target phase values. Covariance matrices have been derived that take into account the increased variance and the correlation between the phases at different frequencies that is introduced by the time-zero cancellation method.

REFERENCES

[1] J. Verspecht, F. Verbeyst, and M. V. Bossche, "Network analysis beyond S-parameters: Characterizing and modeling component behaviour under modulated large-signal operating conditions," in *56th ARFTG Conf. Dig.*, Dec. 2000, pp. 9–12.

[2] P. S. Blockley, D. Gunyan, and J. B. Scott, "Mixer-based, vector-corrected, vector signal/network analyzer offering 300 kHz–20 GHz," in *IEEE MTT-S Int. Microw. Symp. Dig.*, Jun. 2005, pp. 1497–1500.

[3] J. Jargon, D. DeGroot, and D. Vecchia, "Repeatability study of commercial harmonic phase standards measured by a nonlinear vector network analyzer," in *62nd ARFTG Microw. Meas. Conf.*, Dec. 2003, vol. 3, pp. 243–258.

[4] K. J. Coakley and P. Hale, "Alignment of noisy signals," *IEEE Trans. Instrum. Meas.*, vol. 50, no. 1, pp. 141–149, Feb. 2001.

[5] C. D. Woody, "Characterization of an adaptive filter for the analysis of variable latency neuroelectric signals," *IEE Med. Biol. Eng. Comput.*, vol. 5, pp. 539–553, 1967.

[6] J. Jargon, D. DeGroot, K. Gupta, and A. Cidronali, "Calculating ratios of harmonically related, complex signals with application to nonlinear large-signal scattering parameters," in *60th ARFTG Conf. Dig.*, Dec. 2002, pp. 113–122.

[7] F. Verbeyst, 2006, Private communication. *Note*: F. Verbeyst and M. Vanden Bossche are with NMDG Engineering and J. Verspecht is with Jan Verspecht bvba..

[8] *Guide to the Expression of Uncertainty in Measurement*. Genve, Switzerland: Int. Org. Standard., 1995.

[9] K. A. Remley, D. F. Williams, D. M. M.-P. Schreurs, G. Loglio, and A. Cidronali, "Phase detrending for measured multisine signals," in *61th ARFTG Conf. Dig.*, Jun. 2003, pp. 73–83.

[10] G. Loglio, J. Jargon, and D. C. DeGroot, "Phasor angle definition suitable for intermodulation measurements," in *65th ARFTG Conf. Dig.*, Jun. 2005, pp. 83–89.

[11] T. Nakatani, T. Matsuura, and K. Ogawa, "A simple method for measuring the IM3 components of multi-stage cascaded power amplifiers considering the phase characteristics," in *IEEE MTT-S Int. Microw. Symp. Dig.*, Jun. 2004, vol. 3, pp. 1731–1734.

[12] J. P. M. Jose, C. Pedro, and P. M. Cabral, "New method for phase characterization of nonlinear distortion products," in *IEEE MTT-S Int. Microw. Symp. Dig.*, Jun. 2005, pp. 971–974.

[13] P. Blockley, D. Gunyan, and J. B. Scott, "Wide-bandwidth, vector-corrected measurement with high spurious-free dynamic range," in *65th ARFTG Conf. Dig.*, Jun. 2005, pp. 185–188.

[14] S. J. Press, *Applied Multivariate Analysis*. New York: Holt, Rinehart and Winston, 1972, p. 63.

[15] B. D. Hall, "Calculating measurement uncertainty for complex-valued quantities," *Meas. Sci. Technol.*, pp. 368–375, Feb. 2003.

Peter Stuart Blockley (S'03) received the B.Sc. degree from Macquarie University, Sydney, N.S.W., Australia, in 2002, and is currently working toward the Ph.D. degree at Macquarie University.

He has authored or coauthored five publications. His research activities focus on device characterization and metrology for microwave and millimeter-wave systems.

Mr. Blockley is the chair of the IEEE student branch at Macquarie University. He was the recipient of the 1997 Merit Award in Electronics Technology, the 2005 Automatic RF Techniques Group (ARFTG) Best Interactive Session Paper Award, and the 2005 Macquarie University Innovation Award for work in partnership with Agilent Technologies.

Jonathan Brereton Scott (M'80–SM'99) received the B.Sc., B.E., M.Eng.Sc,. and Ph.D. degrees from The University of Sydney, Sydney, Australia in 1977, 1979, 1986, and 1997, respectively.

Until 1997, he was with the Department of Electrical Engineering, University of Sydney. In 1995, he was a visitor with University College London, and subsequently a Visiting Lecturer with the University of Western Sydney. He was involved in establishing and subsequently teaching in the Graduate Program in Audio of the School of Architectural and Design Science, Sydney University. He was a founding member of the Collaborative Nonlinear Electronic Research Facility (CNERF) of the Electronics Department, Macquarie University. In 1997 and 1998, he was Chief Engineer with RF Technology, Sydney, Australia. He has served on committees of the Standards Association of Australia. He serves on the NRC Review Panel for the National Institute of Standards and Technology (NIST)'s Electronics and Electrical Engineering Laboratory. He is an Honorary Associate of Macquarie University. In 1998, he joined the Microwave Technology Center, Hewlett-Packard (now Agilent Technologies), Santa Rosa, CA, where he was responsible for advanced measurement systems. In 2006, he accepted the Foundation Professorship in Electrical Engineering with the University of Waikato, Hamilton, New Zealand. He has authored or coauthored numerous refereed publications, several book chapters, and a textbook. He holds a number of patents.

Prof. Scott is a Fellow of the Institute of Engineers, Australia and a member of the Audio Engineering Society. In 1993, he held a British Telecom Research Fellowship. He was the recipient of the 1994 Electrical Engineering Foundation Medal for Excellence in Teaching.

Daniel Gunyan (M'97) received the B.S. degree in electrical and computer engineering and M.S. degree in electrical engineering from Brigham Young University, Provo, UT, in 1996 and 1997, respectively.

Since 1997, he has been with Agilent Technologies (formerly Hewlett-Packard), Santa Rosa, CA, where he has been involved in both manufacturing and design of microwave and millimeter-wave components for measurement systems and radio transceivers. He is currently involved with the development of test systems and measurement methods for nonlinear characterization and modeling of high-frequency devices, components, and systems.

Anthony Edward Parker (S'84–M'90–SM'95) received the B.Sc., B.E., and Ph.D. degrees from The University of Sydney, Sydney, Australia, in 1983, 1985, and 1992, respectively.

In 1990, he joined Macquarie University, Sydney, N.S.W., Australia, where he is a Professor of microwave device and circuit research within the Department of Electronics. He has a continuing project on characterization of microwave devices and design of low-distortion communications circuits. He has consulted with several companies including M/A-COM, Lowell, MA, and Agilent Technologies, Santa Rosa, CA. He is Director of the Collaborative Nonlinear Electronic Research Facility (CNERF), Macquarie University. He has developed accurate circuit simulation techniques, such as used in field-effect transistor (FET) and high electron-mobility transistor (HEMT) models. He has authored or coauthored over 120 publications. His recent research has been in the area of intermodulation in broadband circuits and systems, including a major project with Mimix Broadband Inc.

Prof. Parker is a member of the Institution of Engineering and Technology, U.K., the Institution of Engineers, Australia, and the Information and Telecommunications and Electronic Engineers Society, Australia. He is also a committee member of the IEEE Antennas and Propagation (AP)/Microwave Theory and Techniques (MTT) N.S.W. Local Chapter.